Electronic structure and magnetism of one-dimensional Fe monatomic wires on Au(788) investigated with ARPES and XMCD

Hideki Fujisawa,[1] Susumu Shiraki,[2] Masashi Furukawa,[1] Shintaro Ito,[2] Tetsuya Nakamura,[3] Takayuki Muro,[3] Masashi Nantoh,[1,*] and Maki Kawai[1,2,4,†]

[1]*RIKEN (The Institute of Physical and Chemical Research), 2-1 Hirosawa, Wako, Saitama 351-0198, Japan*

[2]*Graduate School of Frontier Sciences, The University of Tokyo, 5-1-5 Kashiwanoha, Kashiwa, Chiba 277-8561, Japan*

[3]*Japan Synchrotron Radiation Research Institute (JASRI), SPring-8, 1-1-1 Kouto, Mikazuki, Sayo, Hyogo 679-5198, Japan*

[4]*CREST, Japan Science and Technology Agency (JST), 4-1-8, Honcho, Kawaguchi, Saitama 332-0012, Japan*

(Received 16 April 2007; published 20 June 2007)

In this study of fabricated one-dimensional (1D) monatomic Fe wires on a Au(788) substrate, electronic and magnetic features are investigated by angle-resolved photoemission spectroscopy (ARPES) and x-ray magnetic circular dichroism (XMCD). The ARPES spectra show little dispersion both in the parallel and perpendicular directions to the wires revealing a strongly localized nature of the Fe $3d$ electrons. Finite intensity of the XMCD signals has angular dependence reflecting an anisotropic feature of the localized magnetic moments with an easy axis perpendicular to the substrate. Temperature and field dependence of the XMCD signals shows superparamagnetic behavior well described by the 1D Ising model exhibiting large hysteresis below the blocking temperature, which is ruled by the anisotropy energy. Increase of the average size of the spin blocks with reduced temperature enhances the dramatic change of the magnetic properties of the 1D spin system from soft to hard within a narrow temperature range.

DOI: 10.1103/PhysRevB.75.245423 PACS number(s): 73.90.+f, 75.25.+z, 75.20.−g, 75.30.Gw

I. INTRODUCTION

Magnetism in a one-dimensional (1D) system is a classical but still the latest problem in condensed matter physics. Because of simplicity and fewer parameters of the system, this problem has been treated in theoretical works early in the 20th century. It has been proved that ferromagnetism cannot be caused by localized magnetic moments ordered in one dimension even in the case that the Ising model, which is more favorable for a ferromagnetic ground state than the x-y model or the Heisenberg model, can be applied.[1] This is understandable by intuition if we consider that quantum and thermal fluctuation effects are enhanced in the 1D system.

On the other hand, itinerant-electron ferromagnetism in the 1D electron system is prohibited by the Lieb-Mattis theorem, which starts with the general Hamiltonian.[2] However, recent theoretical works have found that ferromagnetic ground states appear if strict one dimensionality is broken by orbital degeneracy[3] or by quasi-1D geometry like coupled chains[4] or a trestle.[5] Furthermore, the possibility of atomic-scale ferromagnets has been pointed out regarding the adsorbate wires in specific atomic arrangements[6] since they have a flatband near the Fermi level (E_F), which has been proved to cause ferromagnetism in some specific lattices (a bipartite lattice, the Kagomé lattice, etc.) with specific electron fillings.[7] These results seem to reflect the fact that strong on-site Coulomb repulsion U and high density of states near the Fermi level $N(E_F)$, which occur in the 1D systems, are basically advantageous to fulfill the Stoner criterion >1.[8]

Recent progress in surface characterization and metal deposition techniques has made it possible to fabricate artificial 1D structures in self-organized growth manners.[9] Consequently, experimental confirmation about ferromagnetism in the 1D system has been attempted.[10] Extensive studies have been focused on monolayer stripes, and dipolar superferromagnetism has been discovered on Fe/W(110),[11] while nonequilibrium superparamagnetism has been observed on Fe/Cu(111) (Ref. 12) and Fe/Au(111).[13] In the case of these quasi-1D structures, the ferromagnetic order in each stripe can be explained within the limit of the two-dimensional Ising model. Accordingly, further interest is focused on the strictly 1D system, in which the magnetism of each wire or chain is the main research subject. Recently, Gambardella *et al.* have successfully observed the magnetism of monatomic Co chains constructed on a Pt(997) substrate.[14] It has been found that enhanced magnetic moments showing out-of-plane anisotropy exhibit a long-range ferromagnetically ordered state below 15 K, which corresponds to the blocking temperature in superparamagnetism.

In this study, we investigate the electronic structure and magnetism of 1D monatomic Fe wires fabricated on Au(788) by angle-resolved photoemission spectroscopy (ARPES) and x-ray magnetic circular dichroism (XMCD). ARPES results show a strongly localized nature of Fe $3d$ electrons, while XMCD measurements reveal out-of-plane anisotropy of the localized magnetic moments. Field and temperature dependence of the XMCD signal indicates superparamagnetic behavior expected in the 1D Ising system. We found that the increase of the average length of the spin blocks with reduced temperature causes overshoot of the spin-relaxation time resulting in a dramatic change of the magnetic properties at the blocking temperature.

II. EXPERIMENT

For the substrates, we employed Au(788) crystals, which exhibit a thermally stable vicinal facet with respective angle of 3.5° and terrace width of 39 Å. The sample surface was prepared by extensive sputtering-annealing cycles in the

ultrahigh-vacuum chamber until low-energy electron diffraction patterns displayed the characteristic spot splitting. Fe was deposited with an electron-beam evaporator at room temperature (RT). The Fe coverage was controlled by calibration with a quartz-crystal film-thickness monitor and shutter control. Scanning tunneling microscopy (STM) observations were performed *in situ* after the depositions to confirm the actual Fe coverage. ARPES measurements were carried out with He Iα radiation at RT. XMCD experiments were performed using synchrotron radiation of the soft x-ray beamline BL25SU at SPring-8 in Harima, Japan. In the beamline, circular polarized soft x-ray from a twin helical undulator was monochromatized and focused on the sample through pinholes of a permanent magnet circuit. Fe $2p \rightarrow 3d$ x-ray-absorption spectroscopy (XAS) spectra were measured by the total electron yield method in which the sample current is directly measured while scanning the photon energy.

III. RESULTS AND DISCUSSION

Our previous STM studies have revealed the structural features and the formation mechanism of the Fe atomic wires.[15] At the initial stage of the step decoration, Fe atoms substitute for Au at the step edge sites located, with regular spacing, at the fcc stacking regions of the $22\times\sqrt{3}$ surface reconstruction structure of Au(111) terraces. As the Fe coverage is increased, these exchange sites act as nucleation centers and create evenly spaced Fe fragments aligned along the steps, which are finally connected with each other forming monatomic wires. The second rows start their growth at the same periodic positions.

At the Fe coverage of 0.08 ML, an array of the first atomic rows is formed and the second row growth just begins; hence, the wires are composed of monatomic wires and short segments of double atomic wires arranged alternately with the same periodicity as the nucleation sites. This secures the connections between the fragments and one dimensionality of the system, and excludes the possibility that long-range ferromagnetic order was prohibited due to the short length of the wire pieces. All the experiments in this study were performed at the same Fe coverage.

The ARPES measurements have been performed in both parallel and perpendicular directions to the steps and the Fe wires fabricated along them. As we reported in the previous papers,[15] the spectra measured in the perpendicular direction show little dispersion owing to the confinement of the Fe 3*d* electrons in the 1D wires. Originally, we expected that the spectra measured in the parallel direction were more dispersive than those in the perpendicular direction, reflecting the interaction between the Fe 3*d* orbitals. Contrary to our expectation, the spectra measured in both directions indicate basically the same behavior. This suggests weak intercoupling between the 3*d* orbitals on the adjacent Fe atoms.

Figures 1(a) and 1(b) demonstrate the band dispersion relations obtained from the ARPES spectra measured in the parallel direction on clean Au(788) and 0.08 ML Fe/Au(788), respectively. The bands showing parabolic dispersion are the Au 6*s* surface state and the bulk states, which

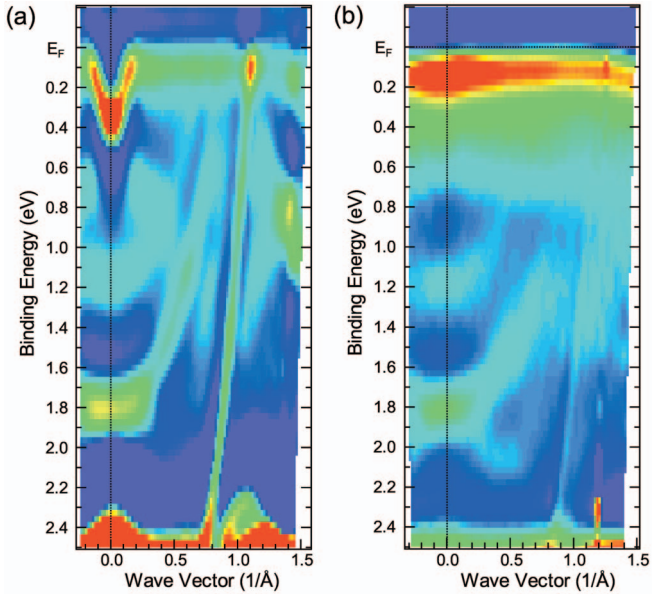

FIG. 1. (Color) Band dispersion relations obtained from the ARPES spectra measured in the parallel direction to the steps on (a) clean Au(788) and (b) 0.08 ML Fe/Au(788). The ARPES measurements were performed at RT with He Iα radiation at normal incidence. The second derivative of the spectral intensity is plotted.

were clearly observed on the clean Au(788). On the 0.08 ML Fe/Au(788), a characteristic flatband is observed just below E_F. Considering the large photoionization cross section of the Fe 3*d* orbitals at the present photon energy,[16] this represents the Fe 3*d* electronic states. Little dispersion observed even in the parallel direction implies that the Fe 3*d* electrons are localized on each atomic site, and the hybridization between the Fe 4*s* and the Fe 3*d* orbitals is negligible. This is reasonable since the lattice constant of 2.75 ± 0.1 Å on the $22\times\sqrt{3}$ reconstructed Au(111) surface,[17] where the Fe wires grow pseudomorphically, is much larger than 2.25 Å of the freestanding Fe monatomic wire obtained by an *ab initio* study,[18] and the 3*d* orbitals decay faster than the 4*s* orbital.

This situation for the Fe 3*d* electrons is probably not very different from isolated Fe atoms in the sea of the Au 6*s* electrons, which act as Kondo impurities. Since the Fe/Au is known as a Kondo system with Kondo temperature (T_K) of $\sim$1.5 K,[19] the *s-d* interaction between the Fe 3*d* and the Au 6*s* electrons is weak but not negligible ($J_{sd}\neq 0$). A possible explanation for our ARPES results is that the Fe 3*d* states form virtual bound states.[20] Since the *s-d* coupling is weak, the density of states of virtual localized level is not so broadened resulting in spin polarization, and the split peak corresponding to the spin-polarized states below E_F gives rise to the localized magnetic moment on each Fe atom.[21]

XMCD measurements have been performed on 0.08 ML Fe/Au(788) to confirm the spin polarization expected from the ARPES results. XAS spectra measured at normal incidence with the photon energy swept across the spin-orbit split Fe L_2 and L_3 absorption edges are given in Fig. 2(a). I_+ and I_- correspond to the absorption intensities with right- and left-circularly polarized light, respectively, taking the direction of the magnetic field as the quantization axis. In this

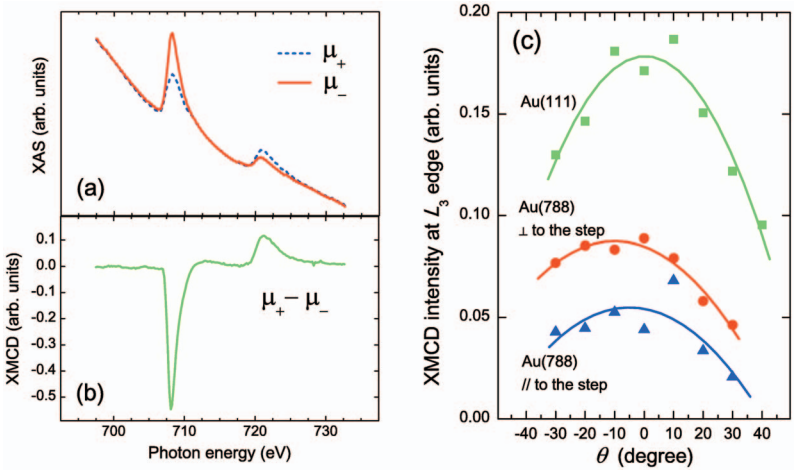

FIG. 2. (Color) XMCD measurements on the Fe monatomic wires in the external magnetic field of 1.9 T. (a) XAS spectra measured at normal incidence with the photon energy swept across the spin-orbit split Fe L_2 and L_3 absorption edges. μ_+ and μ_- correspond to the absorption intensities with right- and left-circularly polarized light, taking the direction of the magnetic field as the quantization axis. (b) XMCD spectrum defined as $\Delta\mu=\mu_+-\mu_-$. The intensity is normalized by the edge jump at the L_3 peak in the XAS spectra. (c) The L_3 peak intensity plotted as a function of the incidence angle θ with respect to the sample normal direction.

study, the XMCD spectrum is defined as $\Delta I=I_+-I_-$, as shown in Fig. 2(b). The strong dichroism observed in the spectra directly proves the existence of the magnetic moments and their alignment in the external field.

It is well known that the local orbital (m_L) and spin (m_S) magnetic moments can be deduced by using the magneto-optical sum rules.[22] Although the number of holes in the 3*d* band is unknown in the present case of the Fe monatomic wires, we can obtain the orbital to spin moment ratio by canceling it,

$$m_L/(m_S-7m_T)=2q/(9p-6q), \tag{1}$$

where m_T is the expectation value of the magnetic dipole operator, and p and q are, respectively, the integrals over L_3 and (L_3+L_2) peaks of the XMCD signal. Using XMCD data shown in Fig. 2(b), we obtained $m_L/(m_S-7m_T)=0.17$. This value is much larger than 0.043 obtained for the bulk bcc Fe.[23] However, it should be noted that the dipolar contribution m_T, which can be neglected in the case of the bulk Fe, is sizable because spin-orbit coupling is not negligible in the low dimensional system. If we use the m_T value of ~0.05 which Ohresser *et al.* reported for Fe clusters on Au(111) with Fe coverage of <0.1 ML,[13] the m_L/m_S value can be corrected down to 0.11, which is still larger than the bulk Fe. This enhancement of the orbital moment is considered as characteristic effect for the low dimensional system due to the lower coordination than the bulk.

Figure 2(c) depicts angular dependence of the XMCD intensity at the L_3 edge, which is proportional to the magnetization. The L_3 peak intensity is plotted as a function of the incidence angle θ with respect to the sample normal direction. Series of measurements were performed in both parallel and perpendicular planes to the wires. Although the plots are somewhat scattered because of the small signal intensity at the Fe coverage of 0.08 ML, it is clear that the intensity has a maximum value around $\theta=0$ indicating an anisotropic feature with an easy axis in the out-of-plane direction.

Generally, magnetic anisotropy can be categorized in three phenomena, i.e., magnetostatic shape anisotropy, magnetoelastic anisotropy, and magnetocrystalline anisotropy. The magnetostatic shape anisotropy is caused by magnetic dipole interaction. In the case of the wire shape, the easy axis must be parallel to the wire. Hence, it is not the present case. The magnetoelastic anisotropy is the opposite phenomenon to magnetostriction. Since the lattice constant of the Au substrate is larger than the freestanding Fe wire, it is natural to think that the Fe wire is expanded, which must align the magnetic moment in line, too. Consequently, the only possible origin of the observed phenomenon is the magnetocrystalline anisotropy. The mechanism is probably twofold. The *s-d* coupling between the Au 6*s* and the Fe 3*d* electrons fixes the orientation of the Fe 3*d* orbitals with respect to the surface. The spin-orbit interaction then fixes the spin direction. As a result, the magnetic moment is fixed to the crystal axis of the substrate.

These ARPES and XMCD results reveal that this system basically fulfills the important premises of the 1D Ising model, in which localized spins arranged in line can take only two opposite (up and down) directions. This secures the applicability of the 1D Ising model to this system to a certain extent if the localized spins are ferromagnetically coupled. As we mentioned, it has been proved that the 1D Ising system cannot have a ferromagnetic ground state.[1] Although this exact solution prohibits long-range ferromagnetic order, the existence of short-range order is not denied.

Now, we focus on the magnetic behavior of the array of the Fe monatomic wires. At various temperatures, we measured the field dependence of the magnetization by plotting the L_3 peak intensity as a function of the external magnetic field (B). The incidence of the polarized light and the direction of the applied magnetic field are both sample normal. Figures 3(a)–3(d) demonstrate the magnetization curves measured at $T=100$, 50, 30, and 18 K, respectively.

The variation of the magnetization curves depending on the temperature can be well understood if we assume superparamagnetism, which is often observed in the assembly of magnetic particles. Below the Curie temperature (T_C), the localized spins are ordered ferromagnetically in short range, and spin blocks of finite length are formed spontaneously. These blocks yielding giant spins behave paramagnetically due to the weak mutual coupling but show the low saturation field resulting in the "Z-shaped" magnetization curve, as typically shown in Fig. 3(c). The appearance of the superparamagnetic phase is direct indication of the collective spin behavior in consequence of the ferromagnetic coupling be-

tween the localized moments on adjacent Fe atoms.

On the other hand, the large hysteresis observed in Fig. 3(d) can be caused by the magnetic anisotropy, which is actually observed in the angular dependence measurements [Fig. 2(c)]. The Néel-Brown model[24] gives the decay of the remanent magnetization as

$$M(t) = M(0)\exp(-t/\tau), \tag{2}$$

where τ is the relaxation time,

$$1/\tau = f\exp(-E_a/k_BT). \tag{3}$$

f is the frequency factor of $\sim 10^{-9}$ s^{-1}, E_a is the average value of anisotropy energy of the spin blocks, and k_B is the Boltzmann constant. When the measurement time is comparable or shorter than τ, a hysteresis loop with finite remanence can be observed. The temperature giving τ comparable to the measurement time is defined as the blocking temperature T_b. We obtained $T_b \sim 30$ K for the Fe monatomic wires.

To clarify the detailed mechanism, we analyze the data using the Langevin function including the anisotropy energy,

$$M = M_{\text{sat}}\frac{\int_0^{2\pi} d\phi \int_0^{\pi} d\theta \sin\theta\cos\theta e^{[NmB\cos\theta + E_a(\sin\theta_0\sin\theta\cos\phi + \cos\theta_0\cos\theta)^2]/k_BT}}{\int_0^{2\pi} d\phi \int_0^{\pi} d\theta \sin\theta e^{[NmB\cos\theta + E_a(\sin\theta_0\sin\theta\cos\phi + \cos\theta_0\cos\theta)^2]/k_BT}}, \tag{4}$$

where θ and ϕ represent the spherical coordinates of the moment with respect to the external field, N is the average number of atoms per spin block, and m and e_a $(=E_a/N)$ are the magnetic moment and anisotropy energy per atom, respectively.[14] Since $\theta_0=0$ under the measurement conditions, Eq. (4) can be reduced to

$$M = M_{\text{sat}}\frac{\int_0^{\pi} d\theta \sin\theta\cos\theta e^{N(mB\cos\theta + e_a\cos^2\theta)k_BT}}{\int_0^{\pi} d\theta \sin\theta e^{N(mB\cos\theta + e_a\cos^2\theta)k_BT}}. \tag{5}$$

Assuming that m and e_a are independent of T, we obtained $Nm=248$, 160, 142, and 137μ_B and $E_a=1.59$, 1.02, 0.91, and 0.88 meV for $T=30$, 50, 80, and 100 K, respectively, by fitting the calculated curves to the data.

It is obvious that as T increases, the spin blocks become shorter, and thus Nm and E_a decrease. This temperature dependence can be considered as the characteristic feature of the 1D system, which is clearly different from the case of the assembly of magnetic particles, where both Nm and E_a are determined and fixed by the size of the particles. Since the superparamagnetism changes into normal paramagnetism $(N=1)$ gradually, the transition at T_C is indistinct.

This behavior can be understood if we consider a very simple model as follows [Fig. 4(a)]. The Hamiltonian of the 1D Ising system is

$$H = -J\sum_i \sigma_i\sigma_{i+1}, \tag{6}$$

where J is the coupling energy between adjacent localized spins $(J>0$ for ferromagnetic coupling), $\sigma_i=+1$ for up spins, and $\sigma_i=-1$ for down spins. Assume the ground state that all the sites have up spins at $T=0$ K without an external field $(B=0)$. As T increases, the blocks composed of down spins appear spontaneously. Since e_a works as an energy barrier to a spin flip, the formation of a spin block of finite length cannot take place at once but progresses site by site. If a thermally activated spin flips to the down direction, it has antiparallel configuration with both adjacent up spins. Equation (6) gives an increase in energy of $4J$ for this event. Because we treat classical type of spins having relatively large moment, the system is supposed to follow the Boltzmann statistics. Therefore, the probability for the event is $\exp(-4J/k_BT)$, and the reciprocal number of the probability $N_0=\exp(4J/k_BT)$ gives the number of sites in series, within which a spin flip is found.[25]

Once a down spin appears, the flip of the adjacent spins does not change the number of boundaries with antiparallel configuration and thus does not increase the coupling energy at all. Therefore, the adjacent spin can flip if it just exceeds the energy barrier corresponding to e_a. This second spin flip has much larger probability since e_a is much smaller than $4J$, and seems to happen easily during the lifetime of the first down spin. Once a dimmer of down spins is formed, it starts to grow until the populations of up spins and down spins become even in order to get the maximum entropy of mixing, which achieves the lowest Helmholtz's free energy (F).[26] Roughly speaking, the blocks of down spins are evenly spaced with the interval of N_0; as a result, the average number of sites of each block becomes a half of it,

$$N(T) \sim N_0/2 = \exp(4J/k_BT)/2. \tag{7}$$

If the external field B $(\neq 0)$ is applied, the spins antiparallel to B begin to flip to get the energy gain of mB, which can happen only at the boundary sites between the spin blocks. Since $4J \gg mB$, the spin flip hardly takes place at the center sites in the blocks. Although the increase of the spins parallel to B reduces magnetic energy, it increases the entropy term of F. Therefore, not all the spins are aligned to B,

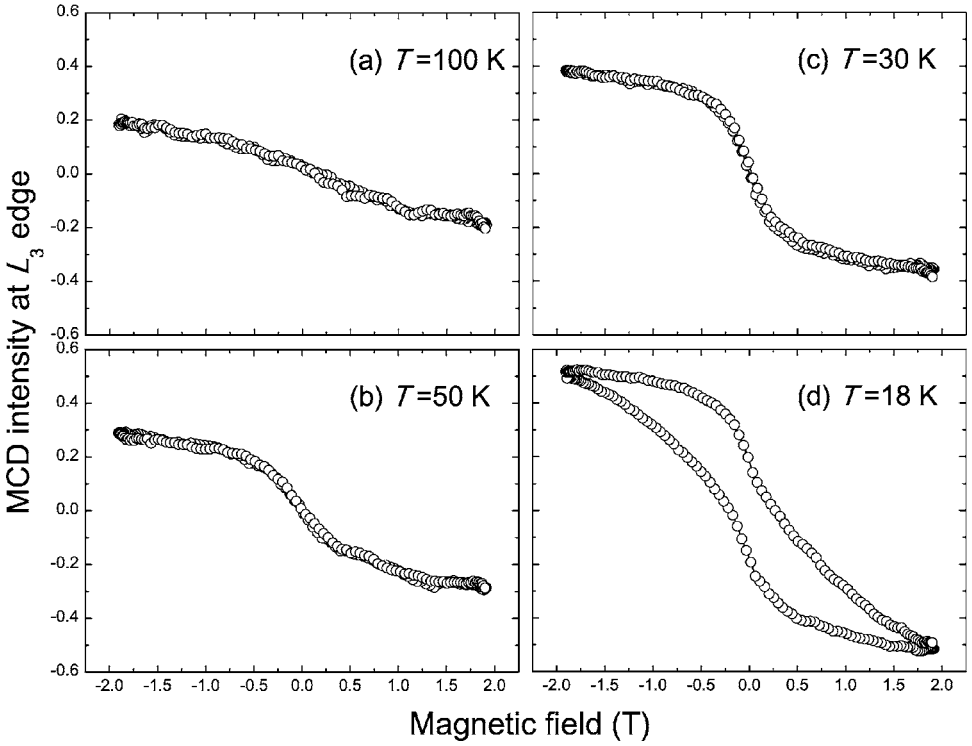

FIG. 3. Typical examples of the magnetization curve measured at T=(a) 100 K, (b) 50 K, (c) 30 K, and (d) 18 K. The L_3 peak intensity is plotted as a function of the external magnetic field B.

but the flip stops when both energy changes are balanced.

Although this model is very simple, Eq. (7) probably gives the correct temperature dependence and order of magnitude, and the discrepancy from Eq. (7) seems to be involved in preexponential factor

$$N(T) = C \exp(4J/k_B T). \quad (8)$$

In Fig. 4(b), $N(T)m$ values are shown in an Arrhenius plot. Based on Eq. (8), the coupling energy is estimated at J =0.55 meV. Pratzer *et al.* have reported J=8.7 meV for Fe monolayer stripes on W(110).[27] Since Fe/W(110) shows dipolar superferromagnetism,[11] it seems to be natural that the J value is much larger than our result. On the other hand, Shen *et al.* have obtained J values of 1.29–2.58 meV for the Fe stripes on Cu(111) which show a superparamagnetic behavior.[12] These values can be normalized into J =0.036–0.19 meV per each atomic wire if divided by the average numbers of atomic rows for the stripes, which we obtained from the Fe coverage of 0.3–0.8 ML and the average terrace width of 100 Å reported in the literature.

Usually, direct exchange interaction is assumed to be the origin of the ferromagnetic coupling between the localized spins in the 1D Ising model. Our STM observations have confirmed that the Fe wires grow pseudomorphically on the Au(111) terraces. It has been also reported that Fe grows in the same manner on W(110) (Ref. 28) and on Cu(111).[29] Accordingly, the nearest-neighbor distance d for the Fe wires and for the monolayer stripes is obtained as d_{Au} =2.75±0.1 Å,[17] d_{W}=2.74 Å, and d_{Cu}=2.56 Å, respectively, on Au(111), W(110), and Cu(111). These values are all larger than d_{Fe}=2.48 Å for the bulk bcc Fe and d_{Fe}=2.25 Å for the freestanding Fe monatomic wire.[18] d_{W} is nearly equal to d_{Au}, although J on W(110) is much larger than the value on Au(111). d_{Cu} is much smaller regardless of the weak coupling expected from the small J values obtained on Cu(111). These facts imply that we cannot discuss the strength of the ferromagnetic coupling just in terms of d.

One possible explanation is that the Fe 3d orbitals have different orientations with respect to the surface depending on the substrate, which changes the orbital overlaps between the adjacent Fe atoms varying the strength of the direct exchange interaction. It is possible that the 3d orbitals of Fe/W(110) have different orientations from those of Fe/Au(111) and Fe/Cu(111), because d-d interaction is dominant on W(110), where 85% of the Fermi level density of states is from W 5d states,[30] while the s-d interaction plays an important role on the noble-metal substrates. This seems to be consistent with the fact that Fe stripes on W(110) indicates in-plane anisotropy,[11] while both of the Fe wires on Au(111) [Fig. 2(c)] and the Fe stripes on Cu(111) (Ref. 12) exhibit out-of-plane anisotropy.

However, even if taking into account the fact that the orbital overlaps between the adjacent Fe atoms depend on d and the orbital orientation, it is still not understandable that J on Cu(111) is comparable or even smaller compared to the value on Au(111). If the Fe 3d orbitals have the same orientation both on Cu(111) and on Au(111), $d_{\mathrm{Cu}} \ll d_{\mathrm{Au}}$ must have given the larger J on Cu(111). It is likely that the magnetic coupling on the noble-metal substrates is not simply caused by the direct exchange but has multiple origins. Another possible mechanism for the coupling is the Ruderman-Kittel-Kasuya-Yoshida (RKKY) interaction intermediate by the s electrons of the substrate.[31] In this case, the coupling energy J_{RKKY} is proportional to a function $G(2k_F r)$ of the Fermi wave vector of the s electrons (k_F) and the distance between the localized spins (r),

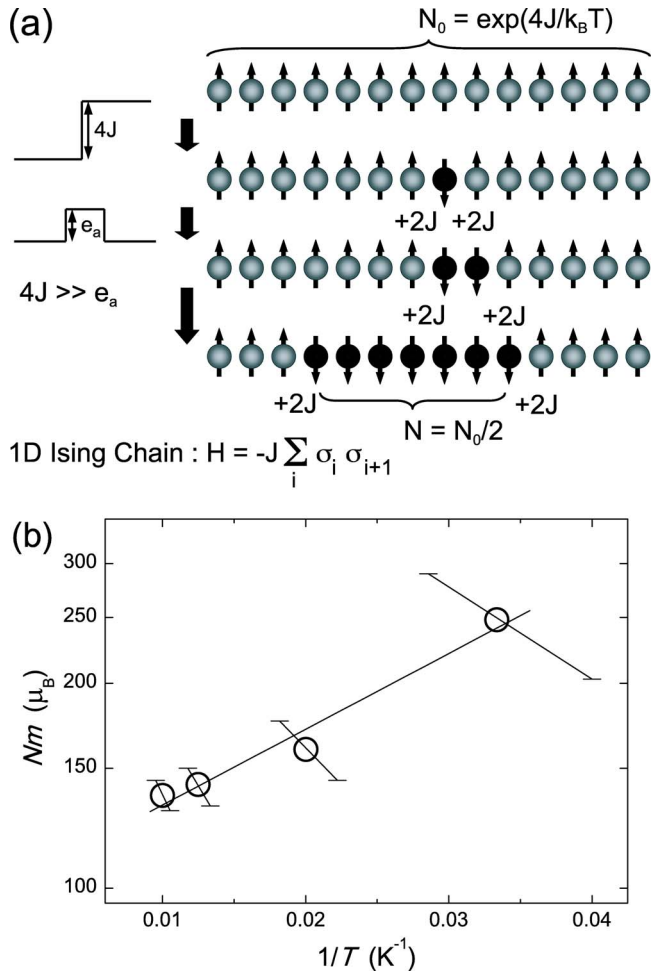

FIG. 4. (Color online) (a) Schematic diagram of the formation process of the spin blocks. (b) Temperature dependence of the average size of the spin blocks obtained by fitting the Langevin function to the magnetization curves. The error bars come from the temperature measurement error of ±5° at the sample holder.

$$J_{\mathrm{RKKY}} \propto |J_{sd}|^2 \frac{2k_F r\cos(2k_F r) - \sin(2k_F r)}{(2k_F r)^4} = |J_{sd}|^2 G(2k_F r). \tag{9}$$

$G(2k_Fr)$ is the oscillation function with the period corresponding to the half of the Fermi wavelength $\lambda_F/2$ and decays rapidly as r increases. Therefore, the interaction between the nearest neighbors is dominant, and thus r can be fixed to d_{Fe} which coincides with d of the substrate. Since the (111) planes of the noble metals have surface states, we have to consider both effects through the surface-state electrons and the bulk state electrons.

On Au(111), $r=2.75\pm0.1$ Å,[17] the k_F values are 0.153 and 0.177 Å^{-1} for the spin-split surface-state bands[32] and 1.21 Å^{-1} for the bulk state,[33] respectively. Using these values, Eq. (9) gives $G(2k_Fr)=-0.338$ for the surface state and $G(2k_Fr)=0.002\,98$ for the bulk state, which means that the surface state causes antiferromagnetic coupling while the bulk state gives ferromagnetic one. Basically, similar result is obtained on Cu(111), $G(2k_Fr)=-0.284$ for the surface state and $G(2k_Fr)=0.002\,04$ for the bulk state, using $r=2.56$ Å, $k_F=0.205$ Å^{-1} for the surface,[34] and $k_F=1.36$ Å^{-1} for the bulk.[33] Since the interaction at the surface is mainly subject to the surface-state electrons, it is concluded that antiferromagnetic coupling is caused by the RKKY mechanism in these systems.

As expressed in Eq. (9), J_{RKKY} is also proportional to $|J_{sd}|^2$. The s-d coupling is related to the Kondo temperature as

$$k_B T_K \sim D\exp(-1/2J_{sd}\rho_0), \tag{10}$$

where D is the bandwidth and ρ_0 is the density of states of the conduction band of the host metal.[35] Since the Kondo temperature of the Fe/Cu system is ~24 K,[19] which is much higher than ~1.5 K of the Fe/Au system, J_{sd} seems to have the larger value on Cu(111) than on Au(111). Consequently, the larger $|J_{sd}|^2$ value is considered to bring about the larger J_{RKKY} on Cu(111). If we assume that the total magnetic coupling is given as the sum of the direct exchange interaction and the RKKY interaction, it is likely that the direct exchange is weakened by the RKKY, yielding the weak ferromagnetic coupling between the Fe atoms on Au(111) and Cu(111). Although the small d_{Cu} of 2.56 Å gives relatively strong direct exchange on Cu(111), it is probably canceled by the strong RKKY; as a result, the weak ferromagnetic coupling may remain.

It should be noted that the magnetic property obtained at $T \ll T_b$ is almost equivalent to ferromagnetism since the relaxation time becomes a huge value. Using the relation $E_a = Ne_a$ and $N(T_1)/N(T_2)=\exp(4J/k_BT_1)/\exp(4J/k_BT_2)$ for $T_1=18$ K and $T_2=30$ K, we obtained E_a of 2.8 meV at 18 K. Equation (3) thus gives $\tau \sim 10^{10}$ s, i.e., hundreds of years. The coercive force obtained at 18 K is 2000 times as large as that of the bulk Fe (~1 Oe) and even larger compared to some of the permanent magnets such as KS steel, MK steel, and Alnico 5. In this sense, this system can be considered as a hard magnetic material at 18 K. On the other hand, the magnetization curve measured at 30 K shows typical behavior of a soft magnetic material without hysteresis and remanent magnetization. It is interesting that the sharp transition from hard magnetic to soft magnetic properties takes place within the narrow temperature range of ~12°. This phenomenon originates from the fact that $N(T)$ $[\propto\exp(4J/k_BT)]$ increases exponentially as T decreases and hence E_a $(=Ne_a)$ changes in the same manner, which causes divergent increase of $\tau[\propto\exp(E_a/k_BT)]$ below T_b.

Finally, our result and the previous report on Co/Pt(997) (Ref. 14) seem to support the theoretical prediction that the 1D Ising system cannot have the ferromagnetic ground state.[1] However, this does not deny the itinerant-electron ferromagnetism of the 1D electron system.[3–7] The 1D ferromagnet may be possible if the itinerancy is given to the d electrons by increasing the overlaps between the d orbitals, which is possibly achieved by depositing $4d$ or $5d$ metals with the larger orbital radii or employing the different substrates with the shorter lattice constants such as Cu, Ag, or the different facets of Au.

IV. CONCLUSION

We have fabricated 1D Fe monatomic wires on Au(788) by the step decoration technique and investigated electronic and magnetic properties by ARPES and XMCD measurements. It has been found that the Fe 3*d* electrons form virtual bound states, which yield localized spins on the Fe atomic sites. The localized magnetic moment has the enhanced orbital to spin moment ratio of ~0.11 and shows magnetocrystalline anisotropy with an out-of-plane easy axis. To be consistent with the theoretical prediction based on the 1D Ising model, the Fe monatomic wires do not show a ferromagnetic ordered state but exhibit a superparamagnetic behavior. The magnetization curve indicates large hysteresis arising from pinning of the localized spins by the strong anisotropy, which vanishes at the blocking temperature of ~30 K. Based on a simple model and the data analysis using the Langevin function, we conclude that the average size of spin blocks decreases exponentially with elevated temperature and estimate the ferromagnetic coupling energy at 0.55 meV. We speculate that the ferromagnetic coupling of this system is caused as a result of the competition between the direct exchange and the RKKY interactions. The same temperature dependence of the anisotropy energy per spin-block brings about the colossal change of the spin-relaxation time of the order of $\sim 10^{10}$ within the narrow temperature range of ~12°, which enhances the dramatic transition of the magnetic properties of this 1D spin system.

ACKNOWLEDGMENTS

The synchrotron radiation experiments were performed at SPring-8 with the approval of JASRI as Nanotechnology Support Project (Proposal No. 2006B1567/BL No. 25SU). This research work is partially supported by the Grant-in-Aid for Scientific Research (No. 18350078) and by CREST (Core Research for Evolutional Science and Technology), JST.

*Electronic address: nantoh@riken.jp
†Electronic address: maki@riken.jp

[1] E. Ising, Z. Phys. **31**, 253 (1925).
[2] E. Lieb and D. Mattis, Phys. Rev. **125**, 164 (1962).
[3] J. E. Hirsch, Phys. Rev. B **56**, 11022 (1997); T. Momoi and K. Kubo, *ibid.* **58**, R567 (1998).
[4] S. Liang and H. Pang, Europhys. Lett. **32**, 173 (1995).
[5] S. Daul and R. M. Noack, Phys. Rev. B **58**, 2635 (1998).
[6] S. Watanabe, M. Ichimura, T. Onogi, Y. A. Ono, T. Hashizume, and Y. Wada, Jpn. J. Appl. Phys., Part 2 **36**, L929 (1997).
[7] E. H. Lieb, Phys. Rev. Lett. **62**, 1201 (1989); A. Mielke, J. Phys. A **24**, L73 (1991); H. Tasaki, Phys. Rev. Lett. **69**, 1608 (1992).
[8] E. C. Stoner, Rep. Prog. Phys. **11**, 43 (1946).
[9] H. Röder, E. Hahn, H. Brune, J.-P. Bucher, and K. Kern, Nature (London) **366**, 141 (1993).
[10] F. J. Himpsel, J. E. Ortega, G. J. Mankey, and R. F. Willis, Adv. Phys. **47**, 511 (1998).
[11] H. J. Elmers, J. Hauschild, H. Höche, U. Gradmann, H. Bethge, D. Heuer, and U. Köhler, Phys. Rev. Lett. **73**, 898 (1994); J. Hauschild, H. J. Elmers, and U. Gradmann, Phys. Rev. B **57**, R677 (1998).
[12] J. Shen, R. Skomski, M. Klaua, H. Jenniches, S. S. Manoharan, and J. Kirschner, Phys. Rev. B **56**, 2340 (1997); P. Ohresser, G. Ghiringhelli, O. Tjernberg, N. B. Brookes, and M. Finazzi, *ibid.* **62**, 5803 (2000).
[13] P. Ohresser, N. B. Brookes, S. Padovani, F. Scheurer, and H. Bulou, Phys. Rev. B **64**, 104429 (2001).
[14] P. Gambardella, A. Dallmeyer, K. Maiti, M. C. Malagoli, W. Eberhardt, K. Kern, and C. Carbone, Nature (London) **416**, 301 (2002).
[15] S. Shiraki, H. Fujisawa, M. Nantoh, and M. Kawai, Phys. Rev. Lett. **92**, 096102 (2004); S. Shiraki, H. Fujisawa, M. Nantoh, and M. Kawai, J. Phys. Soc. Jpn. **74**, 2033 (2005).
[16] J. J. Yeh and I. Lindau, At. Data Nucl. Data Tables **32**, 1 (1985).
[17] J. V. Barth, H. Brune, G. Ertl, and R. J. Behm, Phys. Rev. B **42**, 9307 (1990).
[18] D. Spišák and J. Hafner, Phys. Rev. B **65**, 235405 (2002).
[19] K. H. Fischer, in *Electronic Transport Phenomena*, Landolt-Börnstein, New Series, Group III, Vol. 15, Pt. A, edited by K.-H. Hellwege (Springer-Verlag, Berlin, 1982), pp. 300–305.
[20] J. Friedel, Nuovo Cimento, Suppl. **7**, 287 (1958); P. W. Anderson, Phys. Rev. **124**, 41 (1961).
[21] N. Papanikolaou, N. Stefanou, R. Zeller, and P. H. Dederichs, Phys. Rev. B **46**, 10858 (1992).
[22] B. T. Thole, P. Carra, F. Sette, and G. van der Laan, Phys. Rev. Lett. **68**, 1943 (1992); P. Carra, B. T. Thole, M. Altarelli, and X. Wang, *ibid.* **70**, 694 (1993).
[23] C. T. Chen, Y. U. Idzerda, H.-J. Lin, N. V. Smith, G. Meigs, E. Chaban, G. H. Ho, E. Pellegrin, and F. Sette, Phys. Rev. Lett. **75**, 152 (1995).
[24] L. Néel, Ann. Geophys. (C.N.R.S.) **5**, 99 (1949); W. F. Brown, Phys. Rev. **130**, 1677 (1963).
[25] If the system did not have the magnetic anisotropy, single boundary between up and down spins can be formed independently by twisting the 1D chain. In such a case, the probability of the boundary formation is given as $\exp(-2J/k_BT)$, and the average number of the spin blocks is inversely obtained by $N(T) = \exp(2J/k_BT)$, as is often discussed elsewhere.
[26] F $(=E-TS)$ can be minimized if the entropy of mixing between up and down spins $S=-N_0k_B([N(T)/N_0]\ln[N(T)/N_0]+[1-N(T)/N_0]\ln[1-N(T)/N_0])$ has the maximum value, which is obtained with $N(T)=N_0/2$.
[27] M. Pratzer, H. J. Elmers, M. Bode, O. Pietzsch, A. Kubetzka, and R. Wiesendanger, Phys. Rev. Lett. **87**, 127201 (2001).
[28] U. Gradmann and G. Waller, Surf. Sci. **116**, 539 (1982); M. Przybylski and U. Gradmann, J. Appl. Phys. **63**, 3652 (1988).
[29] Y. Darici, J. Marcano, H. Min, and P. A. Montano, Surf. Sci. **195**, 566 (1988); D. Tian, F. Jona, and P. M. Marcus, Phys. Rev. B **45**, 11216 (1992).
[30] D. A. Papaconstantopoulos, *Handbook of the Structure of Elemental Solides* (Plenum, New York, 1986).
[31] M. A. Ruderman and C. Kittel, Phys. Rev. **96**, 99 (1954); T. Kasuya, Prog. Theor. Phys. **16**, 45 (1956); K. Yoshida, Phys. Rev. **106**, 893 (1957); **107**, 396 (1957).

[32] S. LaShell, B. A. McDougall, and E. Jensen, Phys. Rev. Lett. **77**, 3419 (1996).
[33] N. W. Ashcroft and N. D. Mermin, *Solid State Physics* (Saunders College, Philadelphia, 1976), p. 38.
[34] F. Baumberger, T. Greber, and J. Osterwalder, Phys. Rev. B **64**, 195411 (2001).
[35] A. C. Hewson, *The Kondo Problem to Heavy Fermions* (Cambridge University Press, Cambridge, 1993), p. 49.